Craze Initiation and Growth in High-Impact Polystyrene

ATHENE M. DONALD* and EDWARD J. KRAMER, *Department of Materials Science and Engineering and the Materials Science Center, Cornell University, Ithaca, New York 14853*

Synopsis

Quantitative transmission electron microscopy and optical microscopy is used to study craze initiation and growth in thin films of high-impact polystyrene (HIPS). Dilution of the HIPS with unmodified polystyrene reduces the craze–craze interactions, permitting equilibrium growth and craze micromechanics to be studied. It is found that the equilibrium craze length depends on the size of the nucleating rubber particle, but not the internal structure; no short crazes less than a particle diameter are observed. The long crazes can be adequately modelled by the Dugdale model for crazes grown from crack tips. The effects of particle size and particle internal occlusion structure on craze nucleation have been separated. Craze nucleation is only slightly enhanced at highly occluded particles relative to craze nucleation at solid rubber particles of the same size. There is a strong size effect, however, which is independent of particle internal structure. Crazes are rarely nucleated from particles smaller than ~1 μm in diameter, even though these make up about half the total number. These craze nucleation and growth effects may be understood in terms of two hypotheses for craze nucleation: (1) the initial elastic stress enhancement at the rubber particle must exceed the stress concentration at a static craze tip and (2) the region of this enhanced stress must extend at least three fibril spacings from the particle into the glassy matrix. Since the spatial extent of the stress enhancement scales with the particle diameter, the second hypothesis accounts in a natural way for the inability of small rubber particles to nucleate crazes.

INTRODUCTION

Polystrene (PS) can be substantially toughened by the incorporation of rubber particles, to give the polymer known as high-impact polystyrene (HIPS). The role of the rubber particles is to nucleate a large number of crazes, leading to a correspondingly large volume of plastic deformation being formed before failure.[1] However, the details of this toughening mechanism are as yet imperfectly understood. Empirically, manufacturers have established how to obtain a tough polymer, but the exact nature of the rubber particle distribution that yields this optimum material, and why this form of distribution is desirable, are not clear.

It has been shown that the average rubber particle diameter plays an important role[1–3]; the presence of small particles (≤1 μm) alone produces a less tough polymer than if larger particles (2–5 μm) are present, even at constant rubber content.[3] The use of OsO_4 staining in transmission electron microscopy (TEM)[4–7] has demonstrated that the smaller particles tend to be homogeneous, but larger particles contain subinclusions of the glassy matrix. In such occluded particles, each PS occlusion is surrounded by a rubber layer, and the whole

* Present address: Department of Metallurgy and Materials Science, Cambridge University, Cambridge CB23QZ England.

Journal of Applied Polymer Science, Vol. 27, 3729–3741 (1982)
© 1982 John Wiley & Sons, Inc. CCC 0021-8995/82/103729-13$02.30

particle has a rubber outer shell. Interpretation of the apparent size effect is thus complicated by the inhomogeneity of the particles; the effect could be simply due to size or the role of the PS subinclusions could be crucial. The latter possibility has not received much attention in the literature (see, however, Refs. 8 and 9).

Recent experiments[10] have shown that the nature of the internal morphology of the rubber particle has great significance for craze failure. The presence of many small PS subinclusions permits the rubber to fibrillate locally within the particle, to accommodate the deformation of the surrounding craze; the voids produced by this fibrillation are small. An example of a highly occluded particle from which crazes have grown in HIPS is shown in Figure 1(a). The solid rubber particles behave very differently. Elongation along the direction of the tensile axis is accompanied by significant contraction along the equator, generating a large void at the craze-rubber particle interface. Crazes nucleated at a solid rubber particle are shown in Figure 1(b). Since the arguments of fracture mechanics indicate that large voids will be more damaging than small ones, the presence of small unoccluded particles which can generate these large voids should be avoided. A corollary of this line of reasoning is that the optimum

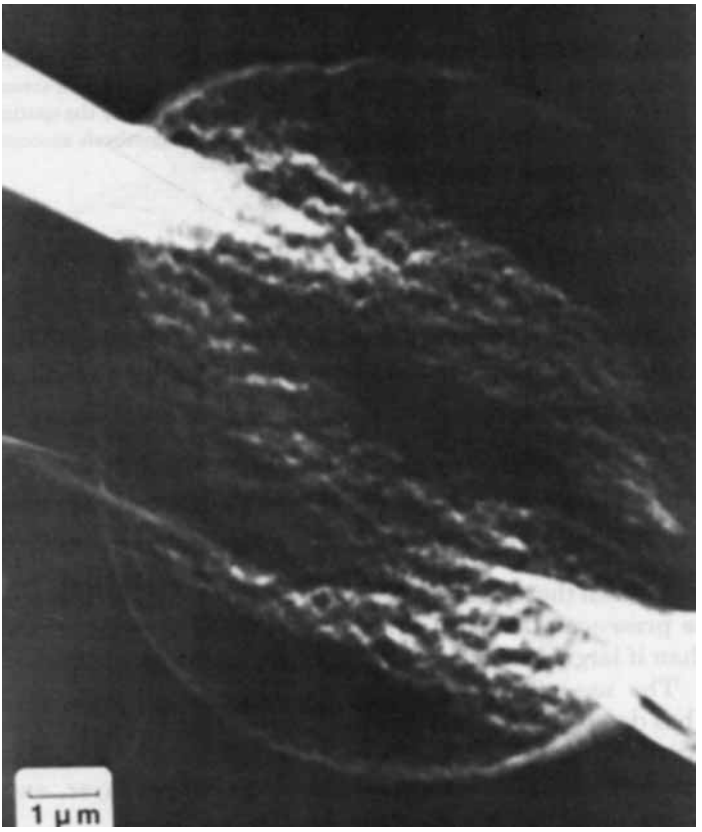

(a)

Fig. 1. (a) A transmission electron micrograph of crazes originating from a highly occluded rubber particle in a thin film of HIPS. (b) A TEM image of crazes originating at a solid rubber particle in a thin film of HIPS.

morphology for rubber particles is likely to consist of many small occlusions rather than a coarse internal particle structure.

These experiments on craze breakdown[10] clearly reveal that arguments based on rubber particle size alone are insufficient to explain variations in toughness. Since toughness will also be determined by the ease with which crazes can be nucleated and their subsequent micromechanical properties, it is necessary to question the role of the internal morphology in this context also.

Several studies have considered the overall role of rubber particles in craze initiation, both theoretically and experimentally.[8,9,11–13] The rubber particles act as sites for craze initiation because a stress concentration is set up at their equator when a tensile stress is applied. Since for a homogeneous particle the magnitude of this stress concentration is independent of particle size, however, no explanation for the apparently poorer craze nucleating power of small particles is found by modelling the particles simply as homogeneous spheres. A refinement of the model to allow for the effect of glassy subinclusions on the shear modulus of a composite particle shows that the stress concentration factor is not significantly altered by the inhomogeneity.[8,9] Argon has suggested[11] that additional stress concentrations may arise because the outer shell of rubber particle is not smooth but locally rippled. In this model the effect will be most pronounced for large composite particles, which will consequently be most efficient as craze initiators.

A further complication in understanding the micromechanics of craze initiation and growth in commercial HIPS is caused by the high number density of particles

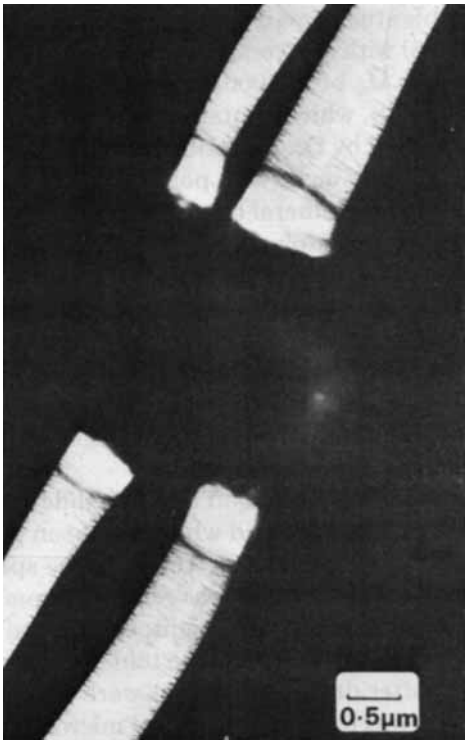

Fig. 1. *(Continued from previous page.)*

with the consequent overlap of their stress fields. This overlap leads to an enhancement of the stress at the particles, the magnitude of this effect being determined by the particle density. The calculations of Oxborough and Bowden[12] indicate significant stress field overlap occurs for a volume fraction of particles greater than 9%. Typical commercial HIPS particle densities exceed this value. By diluting a commercial HIPS with unmodified PS, Oxborough and Bowden[12] investigated craze initiation at isolated rubber particles in a biaxial stress field; reasonable agreement was obtained between the stress levels at which craze initiation occurred experimentally and their predictions. No attempt was made to assess the importance of the internal structure of the particle, the rubber particle being modelled as a homogeneous sphere with the only variables being the ratio of the shear modulus of the particle to that of the matrix and Poisson's ratio of the particle.

In this paper, results are presented from a study of craze initiation and growth in specimens of HIPS diluted with unmodified PS. The consequent low-particle density allows individual crazes to grow effectively unperturbed by other particles and crazes. Combined optical microscopy and TEM then enables the importance of particle internal morphology and particle size to be assessed for craze initiation and growth.

EXPERIMENTAL

Specimen Preparation

The HIPS used in this study was a noncommercial resin containing 10% butadiene rubber (diene-55) with an average particle size of 2.9 μm, in PS of weight average molecular weight $\overline{M}_w$ of 250,000 and number average molecular weight $\overline{M}_n$ of 115,800. This HIPS, which contained no mineral oil commonly added as a plasticizer, was supplied by Dr. R. A. Bubeck of the Dow Chemical Co. The HIPS was diluted to 10% by weight with polystyrene of $\overline{M}_w$ = 300,000 and $\overline{M}_n$ = 124,000, also containing no mineral oil and supplied by Dr. Bubeck.

The polymer mixture was dissolved in toluene and from this solution glass slides were drawn to produce films of thicknesses 0.8, 1.8, and 5 μm. The thinnest films were suitable for quantitative measurements in the transmission electron microscope (TEM), but, for most of the optical studies, thicker films were used. For the thickest film, the thickness was greater than the average particle diameter so that the stress fields of the particles were not significantly perturbed by the free surfaces. The subsequent stages of specimen preparation were identical for the three thicknesses of film.

After the film had dried it was floated off the glass slide onto a water bath, from which it was picked up on a copper grid which had been precoated with a thin film of the solution. To bond the film to the grid, the specimen was exposed briefly to toluene vapor. Excess vapor was removed from the film by placing the specimen in a vacuum desiccator overnight; this procedure ensures that the rubber particles do not remain swollen by the toluene vapor, with a consequent change in properties. After drying specimens were strained in tension in air. The nucleation of crazes was followed by optical microscopy. For those specimens which were subsequently to be characterized by TEM, suitable grid squares were cut from the specimen following straining, and examined in a Siemens 102

electron microscope operating at 125 keV. The copper grid deforms plastically and maintains the level of applied strain in the film while it is examined by TEM. Further details of this specimen preparation technique are described by Lauterwasser and Kramer.[13]

Analysis of Craze Micromechanics

To understand craze growth and the stresses on a craze grown from a rubber particle, it is useful to construct a simple model. The simplest such model is to treat the rubber particle as if it were a crack of length equal to the rubber particle diameter. (This assumption is not as extreme as it sounds. First, because the craze has nucleated from the rubber particle, the tractions across the rubber particle normal to the craze are small due to the low shear modulus of the rubber particle; second because the craze displacements growing from the hypothetical crack rapidly remove the local-stress singularity there and finally because once the craze has propagated more than one rubber particle diameter from the particle, the stress distribution near the craze tip becomes insensitive to the details of the initial stress concentration of the rubber particle and depends strongly only on the local craze surface displacements.) It is then possible to compare experimentally determined craze micromechanical properties with existing theories for crazes at crack tips. These micromechanical properties can be obtained using quantitative TEM.[13] With this technique it is possible to measure the craze surface displacement profile $w(x)$, and from this profile the surface stress profile $S(x)$ can be computed.[14] The craze surface displacements are the displacements of the craze-bulk polymer interfaces as a result of craze growth and thickening; the craze surface stresses are the normal stresses exerted on the craze surfaces by the craze fibrils, averaged over several fibril spacings.

The method for calculating $S(x)$ is based on the distributed dislocation method of Bilby and Eshelby.[15] In this method the actual displacements of the craze are treated as if they were due to a continuous array of dislocations. The linear dislocation density $\alpha(x)$ is related to the displacements by

$$\alpha(x) = -2\frac{dw(x)}{dx} \tag{1}$$

(setting the "Burgers vector" of the fictitious dislocations equal to 1). Physically the stress fields generated by the crack and craze must be such that no stress singularity exists at the crack tip. This requirement leads to a unique solution for the stress profile, and also enables the level of the applied stress α_∞ to be computed. The solution to the problem is given by the equations

$$\sigma_\infty = \frac{E^*}{2\pi}\int_c^a dx\ \alpha(x)\frac{1}{\sqrt{x^2 - c^2}} \tag{2a}$$

and

$$S(x) = \frac{E^*}{2\pi}x\sqrt{x^2 - c^2}\int_c^a \frac{dx_1\alpha(x_1)}{\sqrt{x_1{}^2 - c^2}}\cdot\frac{1}{(x^2 - x_1{}^2)} \tag{2b}$$

where

$$E^* = \begin{cases} E/(1-\nu^2) & \text{plane strain} \\ E & \text{plane stress} \end{cases}$$

and E is Young's modulus, ν is Poisson's ratio, c is the half crack length and a is the total half crack plus craze length. In Eq. (2b), $x > 0$; $S(-x) = S(x)$.

The experimental displacement profile along the craze thickness profile $T(x)$, measured directly from a series of micrographs taken along the craze, and the local value of the volume fraction v_f of the craze.[13] Then

$$w(x) = \tfrac{1}{2}T(x)[1 - v_f(x)]. \tag{3}$$

Values of v_f can be obtained by microdensitometry of the electron image plates. The optical densities of the craze (ϕ_{craze}), the undeformed film (ϕ_{film}), and of a hole through the film (ϕ_{hole}) are measured. The craze volume fraction can then be obtained from the expression

$$v_f = 1 - \frac{\ln(\phi_{\text{craze}}/\phi_{\text{film}})}{\ln(\phi_{\text{hole}}/\phi_{\text{film}})} \tag{4}$$

Knowledge of the forms of the $w(x)$ and $S(x)$ profiles permits a comparison of crazes grown from rubber particles with both theoretical predictions for, and experimental measurements of, crazes grown from crack tips.

The simplest theoretical model applicable to this situation is the Dugdale model.[16,17] In this model, the assumption is made that the craze surface stress is a constant S_c everywhere along the craze. This stress may be computed from measured c and a values to be

$$S_c = \pi\sigma_\infty/[2 \arccos(c/a)] \tag{5}$$

For crazes in unmodified PS, it has been shown[18,19] that the Dugdale model is a reasonable approximation, although stress concentrations do exist at both the craze and crack tips. If crazes at rubber particles can be modelled as crazes at crack tips, the Dugdale model should be equally applicable.

The Dugdale model assumes that the plastic zone is grown from a planar crack. Clearly this is a poor approximation for a rubber particle. However, the analogue of the Dugdale model for a plastic zone growing from a circular hole has been analyzed by Tada.[20] The form of this solution for a hole of radius R_c, with a craze of length a grown from it, is shown in Figure 2. The Dugdale solution for a planar crack of half-length R_c is also shown in this figure. For the case of $(a - R_c)/a > 0.3$, the solutions are identical. Thus for sufficiently long crazes, both models will yield the same solution.

RESULTS

Figure 3 shows the form of the stress profile calculated for a craze grown from a homogeneous rubber particle of radius 1.15 μm using eqs. (2a) and (2b). This profile shows that the craze has very similar micromechanical properties to a craze grown from a crack tip in PS. Over the majority of the craze, the stress is a constant, the level of this stress lying slightly above σ_∞ but below S_c, the stress predicted by the Dugdale model for a craze of the observed length a.

Using optical microscopy to identify those particles which first initiated crazes in a 1.8 μm-thick film, followed by TEM to characterize the internal morphology of these particles, it was found that crazes were only slightly more easily nucleated at occluded particles than at solid rubber particles of the same size. Approximately 19% of those crazes which were generated at the lowest level of strain

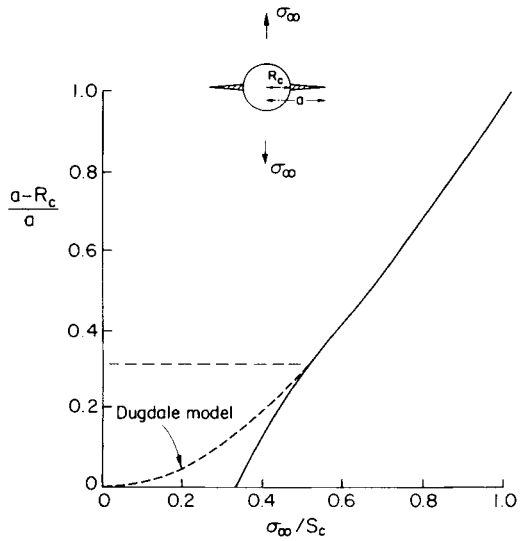

Fig. 2. Predicted length a of a thin yielded zone with constant yield stress S_c growing from a cylindrical void of radius R_c in a thin sheet under an applied stress σ_∞ [after Tada et al.[20]]. The dashed line shows the predictions of the Dugdale model where the zone is assumed to grow from a planar crack of half-length R_c.

nucleated at solid rubber particles, whereas ~25% of the particles in the size range 1.5–2.5 μm, from which most crazes initiated, were solid rubber. Particles larger than 2.5 μm caused significant local increases in the film thickness and were ineffective craze nuclei. Nucleation of crazes by particles with diameters smaller than 1.0 μm, regardless of their internal structure, was rare. The smallest rubber particle observed to nucleate a craze even at the highest strain levels had a diameter 0.8 μm. Since ~50% of the rubber particles smaller than 2.5 μm in this HIPS had diameters smaller than 0.8 μm, these observations indicate the poor craze nucleation by the small rubber particles is a true effect of their size and not due to the variation of their internal structure with size.

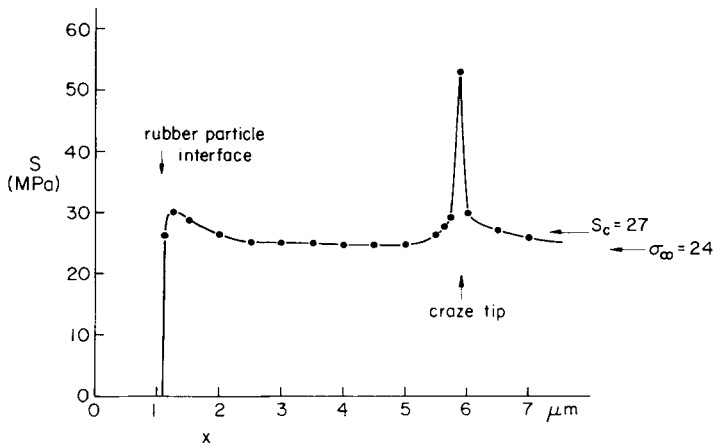

Fig. 3. The surface stress profile along a craze growing from a rubber particle in HIPS. x is the distance from the center of the particle, and the particle radius = 1.15 μm.

For the thick films, where the film thickness (5.5 μm) was greater than the average particle diameter (2.9 μm), it was found that the craze length depended on the diameter of the particle from which it nucleated. This dependence is clear in the optical micrograph of Figure 4(a), and also from the plot of craze length a (measured from the particle center) vs. particle radius in Figure 4(b). There are many short crazes growing from small particles, but the long crazes tend to be nucleated at the larger particles. Those crazes are able to grow to their equilibrium length, in general unperturbed either by other crazes or particles, because the number density of particles in the diluted HIPS is low. In Figure 4(b), only noninteracting crazes are considered. When crazes did intersect other particles, neither optical microscopy nor TEM indicated that particles acted as craze terminators. Note also that, even though there is a large scatter in craze length, no crazes shorter than two particle radii (from the particle center) are observed. This phenomenon, which was observed even at the lowest strain levels, indicates that once crazes are nucleated, they will propagate at least one particle radius from the outer surface of the particle.

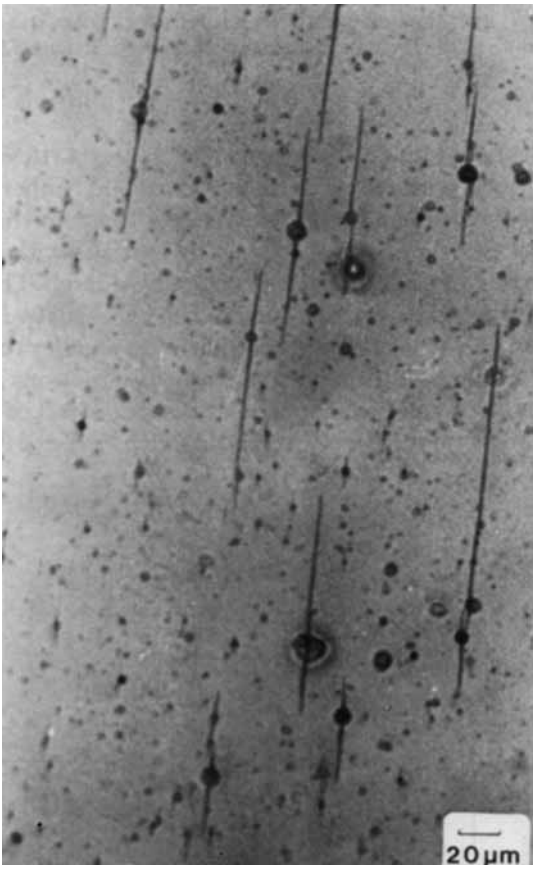

(a)

Fig. 4. (a) Optical micrograph of crazes growing from rubber particles in a diluted HIPS. (b) Craze length a measured from the particle center vs. particle radius. Note that no crazes shorter than two radii are observed, indicated by the dashed line.

DISCUSSION

Craze Growth

The stress profile shown in Figure 3 indicates that crazes grown from rubber particles can be micromechanically modelled as crazes grown from crack tips. It is also clear that the Dugdale model is a reasonable approximation to the craze surface stress profile. Since the Dugdale model is appropriate, the expression it yields relating the crack length c to the craze length a can be applied to predict the length of crazes grown from rubber particles. Equation (5) can be rewritten as

$$\frac{R_c}{a} = \cos\left(\frac{\pi}{2}\frac{\sigma_\infty}{S_c}\right) = K \tag{6}$$

where R_c is an "effective half crack length" for the particle. In this case R_c is not identical to the particle radius since the 3-dimensional nature of the particle must be taken into account. By replacing the actual volume of the particle by an equivalent cylinder of height t (the film thickness) and radius R_c, the problem can be reduced to the 2-dimensional model. Two cases must be considered, one for particles whose actual radius R is less than $t/2$ and one for particles whose R is greater than $t/2$. The solutions for the radius of the equivalent cylinder in these two cases are

$$R_c/t = \pi R^2/2t^2, \quad R < t/2 \tag{7a}$$

and

$$R_c/t = (R^2/2t^2)\,[\pi - 2\cos^{-1}(t/2R)] + \tfrac{1}{2}\sqrt{R^2/t^2 - \tfrac{1}{4}}, \quad R > t/2 \tag{7b}$$

The raw data of Figure 4(b) can now be manipulated to test the predicted variation [eq. (6)] in craze length a with the equivalent particle radius R_c. Figure

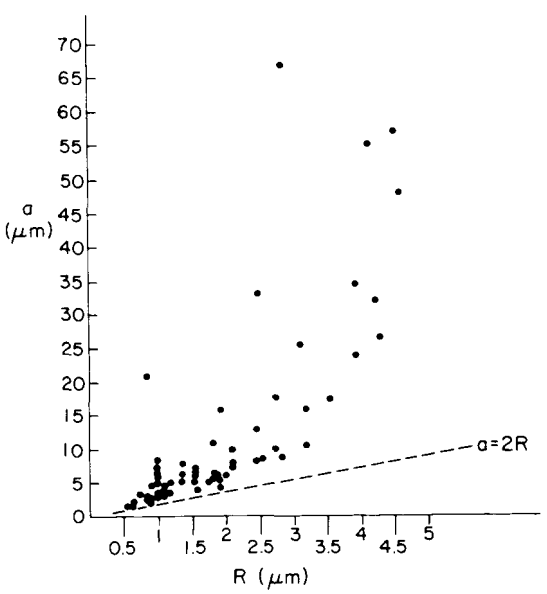

(b)

Fig. 4. *(Continued from previous page)*

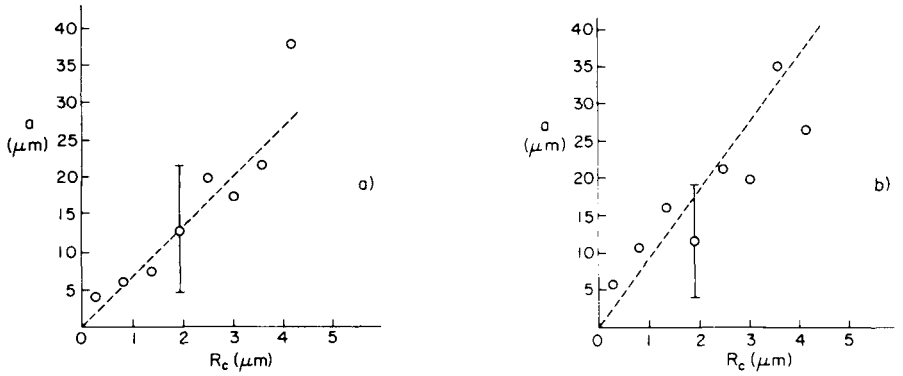

Fig. 5. (a) Average craze length (measured from rubber particle centers) vs. the equivalent particle radius (low applied strain). (b) Same as Figure 5(a) at higher applied strain.

5(a) and 5(b) show the resulting dependence of craze length on the equivalent particle radius R_c. Figure 5(a) shows the same set of data as Figure 4(b), and Figure 5(b) corresponds to a second specimen which had been strained to a higher level. The data are plotted as the average value of a for all particles which fell within a given range of R_c, and typical error bars are shown. Relatively few particles lie at the higher end of the R_c range, and the statistics there are poorer. Lines of best fit to the experimental data are shown.

Figures 5(a) and 5(b) show clearly that there is a marked dependence of a on R_c. There is an appreciable scatter in the experimental data, but the results bear out the linear dependence of craze length on the equivalent particle radius R_c represented by eq. (6). Since for large a/R_c ratios, the constant K in eq. (6) is given by

$$K = \tfrac{1}{2}\pi(1 - \sigma_\infty/S_c)$$

smaller K's and larger slopes of plots of a vs. R_c (Fig. 5) should result from larger applied strains ϵ_∞. The fact that the slope of the line in Figure 5(b) (higher ϵ_∞), corresponding to a ratio $\sigma_\infty/S_c = 0.94$, is higher than that in Figure 5(a) (lower ϵ_∞), corresponding to $\sigma_\infty/S_c = 0.91$, is thus in agreement with these expectations. Because of the high craze density in these samples, however, it is not possible to calculate σ_∞ from the known level of applied strain; consequently, a more quantitative analysis of the change in gradient between Figures 5(a) and 5(b) cannot be made. The rather high craze densities involved also readily explain the scatter in the experimental results. Although craze lengths were only measured for those crazes where no obvious interactions with other crazes or particles had occurred, local variations in the stress field will clearly affect the equilibrium craze lengths. However, despite such variations, it is clear that the basic premise implied by the eq. (6) is correct: Crazes nucleated at rubber particles in HIPS can be reasonably described by the Dugdale model with a consequent linear dependence of craze length a on the effective particle diameter R_c.

Craze Nucleation

The craze nucleation step will be governed by the local elastic stress concentration at the rubber particle equator. Since immediately after nucleation the craze is very thin (it is almost all "tip"), it seems logical to compare the craze nucleation stress concentration with the stress concentration at the craze tip. Certainly a necessary condition (but not a sufficient condition) for craze nucleation is that the local stress concentration at the rubber particle must exceed the stress concentration at the tip of a craze which has grown to its equilibrium length and stopped. Once the craze has nucleated, it will grow in length and width, relieving the stress concentration at the particle (craze base) until this equilibrium length is reached and a stress profile similar to that shown in Figure 3 is achieved.

This hypothesis explains why no crazes are observed to grow to final lengths shorter than a rubber particle diameter from the particle center. If the Dugdale model, or its modification in Figure 2, were literally correct and crazes could be nucleated when the local stress concentration at the particle equator reached S_c, crazes which extend less than $2R$ from the particle center should be observed as σ_∞ is increased. If, however, the average stress on the craze surface must drop from a nucleation stress exceeding that at the craze tip to S_c as the craze grows, exactly the results observed would be expected; no crazes that are short compared to the particle radius would be seen.

An additional requirement for craze nucleation, however, must be fulfilled: The elastic stress concentration must be maintained over a sufficient distance from the particle interface to allow a craze tip with its characteristic structure to develop. It has been shown recently[21] that the craze tip in PS advances by the meniscus instability mechanism in which the void network at the craze tip breaks up into a series of fingers which protrude ahead of the tip, with the polymer fibrils being formed at the webs between the fingers. Typical fibril and finger spacings in PS are 25 nm.[21,22] To satisfy this requirement, a reasonable spatial criterion for the initial nucleating stress distribution would be that the stress enhancement must not drop to less than half its value at the particle surface in less than 3 craze fibril spacings (75 nm in PS).

This second condition provides a reasonable explanation for the effect of rubber particle size on craze nucleation. The initial tensile stress on the equatorial plane outside the particle at a distance x from the particle center may be computed from elasticity theory[23,10,12] and is displayed in Figure 6(a). Although the stress at the particle interface $x = R$ is the same for particles of all sizes, the stress decreases rapidly, approximately as $(R/x)^5$, as x/R increases. The distance $x - R$ from the rubber particle interface in which the stress enhancement falls to half its value at the interface decreases linearly as R decreases; numerically this "decay length" is about one-tenth of the particle diameter.

Figure 6(b) shows the stress concentration at a distance of 3 PS craze fibril spacings ($x - R = 75$ nm) from the rubber particle, as a function of the rubber particle diameter. For particles that are less than 1 μm in diameter, the stress enhancement at this distance is strongly dependent on the particle size, falling rapidly with particle diameter. Particles smaller than 1 μm, therefore, should be poor craze initiators, as is observed. Particles 0.1 μm and smaller in diameter should be completely ineffective at craze nucleation since the stress concentration at the position of the craze tip would be halved before the craze is 10 nm long,

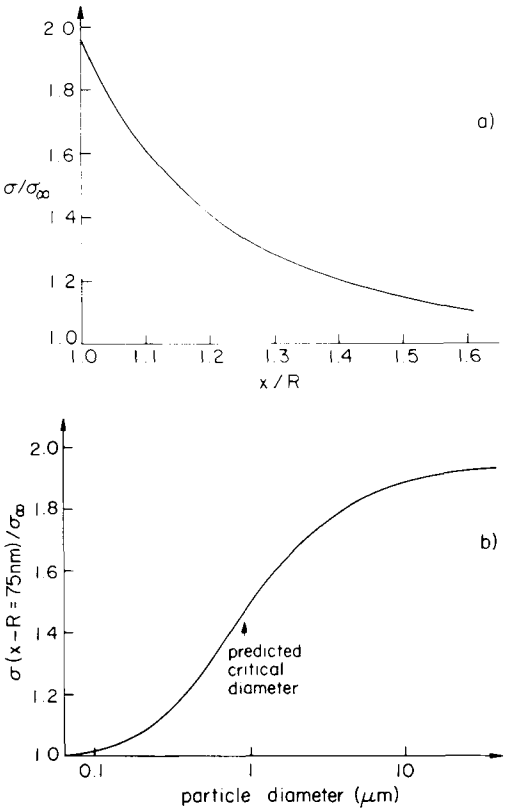

Fig. 6. (a) The stress enhancement in the glassy matrix outside the particle on its equatorial plane as a function of normalized distance from the particle center. x is the distance from the particle center, and R is the particle radius. (b) The stress enhancement at a distance 3 fibril spacings (75 nm) from the particle interface vs. particle diameter.

which is less than *1* fibril spacing. One can not expect such small particles to be any more effective in nucleating crazes than random local fluctuations of density in the homogeneous polymer glass. Experimentally crazes in HIPS or ABS[24] are not nucleated preferentially at such small rubber particles.

While the occlusion structure of the larger particles may well have a slight additional stress concentration as claimed by Argon,[11] the present results demonstrate that the effect of this additional stress concentration on craze nucleation by particles of the same size is small. The more potent craze nucleation of the larger particles is a result primarily of their size and not their occlusion structure. Nevertheless, highly occluded large rubber particles are desirable for another reason; large solid rubber particles [Fig. 1(b)] can break down to form large voids at the craze–particle interface. These large voids grow to become cracks and lead to premature craze (and polymer) fracture. The highly occluded particles are less susceptible to such failure.[8] By considering rubber particle breakdown as well as craze nucleation, one can make a good case for removing all rubber particles in HIPS below the size (~1 μm diameter) that efficiently nucleates crazes. While these particles do not nucleate crazes, they may be intersected by crazes which nucleate at other rubber particles. These intersected particles in turn may breakdown to form relatively large voids which eventually become cracks.

Thus from consideration of both craze initiation and craze break down, it is clear that the greatest improvements in toughness in polymers which deform principally by crazing can be achieved: (1) by minimizing the number of solid rubber particles of all size, (2) by eliminating rubber particles smaller than the critical diameter for craze nucleation, and (3) by introducing particles just larger than the critical diameter (to maximize the total particles that nucleate crazes) which have a large number of very small glassy occlusions.

The financial support of this project through the Cornell Materials Science Center, which is funded by the National Science Foundation is gratefully acknowledged. We especially thank Dr. R. A. Bubeck of Dow Chemical Co. for supplying the noncommercial HIPS and the pure polystyrene used here and for his helpful comments at various stages of this work.

References

1. C. B. Bucknall, *Toughened Plastics*, Applied Science, London, 1977.
2. J. D. Moore, *Polymer*, **12,** 478 (1971).
3. S. G. Turley and H. Keskkula, *Polymer*, **21,** 466 (1980).
4. K. Kato, *J. Electron Microsc.*, **14,** 220 (1965).
5. K. Kato, *Polym. Lett.*, **4,** 35 (1965).
6. M. Matsuo, C. Nozaki, and Y. Jyo, *Polym. Eng. Sci.*, **9,** 197 (1969).
7. P. Beahan, A. Thomas, and M. Bevis, *J. Mater. Sci.*, **11,** 1207 (1976).
8. C. B. Bucknall, *J. Mater. Sci.*, **4,** 214 (1969).
9. T. Ricco, A. Pavan, and F. Danusso, *Polym. Eng. Sci.*, **18,** 774 (1978).
10. A. M. Donald and E. J. Kramer, MSC Report #4535, *J. Mater. Sci.*, to appear.
11. A. S. Argon, *Pure Appl. Chem.*, **43,** 247 (1975).
12. R. J. Oxborough and P. B. Bowden, *Phil. Mag.*, **30,** 171 (1974).
13. B. D. Lauterwasser and E. J. Kramer, *Phil. Mag.*, **39A,** 469 (1979).
14. W. C. V. Wang, Ph.D. thesis, Cornell University, 1981.
15. B. A. Bilby and J. D. Eshelby, *Dislocations and the Theory of Fracture*, H. Liebowitz, Ed., Academic, New York, 1972, Vol. 1, Chap. 2.
16. D. S. J. Dugdale, *Mech. Solids*, **8,** 100 (1960).
17. J. N. Goodier and F. A. Field, *Proceedings of the International Conference on Fracture of Solids*, Met. Soc. Conferences Vol. 20, D. C. Drucker and J. J. Gilman, Eds., Interscience, New York, 1963, p. 103.
18. T. Chan, A. M. Donald, and E. J. Kramer, *J. Mater. Sci.*, **16,** 676 (1981).
19. A. M. Donald, E. J. Kramer, and R. A. Bubeck, MSC Report #4569, *J. Polym. Sci., Polym. Phys. Ed.*, **20,** 1129 (1982).
20. H. Tada, P. Paris, and G. Irwin, *The Stress Analysis of Cracks Handbook*, Del Research Corp., St. Louis, 1973, p. 313.
21. A. M. Donald and E. J. Kramer, *Phil. Mag.*, **434,** 857 (1981).
22. H. R. Brown and E. J. Kramer, *J. Macromol. Sci. Phys.*, **B19,** 487 (1981).
23. J. N. Goodier, *Trans. Am. Soc. Mech. Eng.*, **55,** 39 (1933).
24. A. M. Donald and E. J. Kramer, MSC Report #4570, *J. Mater. Sci.*, **17,** 1765 (1982).

Received October 16, 1981
Accepted March 29, 1982